

UC Irvine

UC Irvine Previously Published Works

Title

Visualizing flat spacetime: Viewing optical versus special relativistic effects

Permalink

<https://escholarship.org/uc/item/59n8n72d>

Journal

American Journal of Physics, 75(6)

ISSN

0002-9505

Authors

Black, Don V.
Gopi, M.
Pajarola, Renato
[et al.](#)

Publication Date

2007-06-01

Supplemental Material

<https://escholarship.org/uc/item/59n8n72d#supplemental>

Peer reviewed

Visualizing Flat Spacetime: Viewing Optical versus Special Relativistic Effects

Don V Black*

*Department of Electrical Engineering and Computer Science,
University of California at Irvine, Irvine, CA 92714*

M. Gopi†

*Department of Information and Computer Sciences,
University of California at Irvine, Irvine, CA 92714*

Frank Wessel‡

*Department of Physics & Astronomy,
University of California at Irvine, Irvine, CA 92714*

Renato Pajarola§

Computer Science Department, University of Zürich, Zürich, Switzerland

Falko Kuester¶

*California Institute for Telecommunications and Information Technology,
University of California at San Diego, La Jolla, CA 92093*

(Dated: January 29, 2007)

Abstract

A simple visual representation of Minkowski spacetime appropriate for a student with a background in geometry and algebra is presented. Minkowski spacetime can be modeled with a Euclidean 4-space to yield accurate visualizations as predicted by special relativity theory. The contributions of relativistic aberration as compared to classical pre-relativistic aberration to the geometry are discussed in the context of its visual representation.

I. INTRODUCTION

This paper presents a Euclidean 4D model that can be used to view and explain Minkowski spacetime without resort to higher mathematics. The simple intuitive method presents the fundamental concepts underlying the Theory of Special Relativity and enables the teacher to lead a student from Euclidean geometry into flat spacetime.

For simplicity, *temporal homogeneity*¹ and a flat² spacetime with no acceleration are assumed, and lighting effects are not considered. Under these conditions flat Minkowski spacetime is Euclidean for an inertial observer. The corresponding model can then be viewed and animated based on 4D raytracing.

Temporal extrusion of an inertial 3D object into 4-space along its normalized velocity 4-vector (worldline), followed by the *Lorentz transformation* (length contraction and time dilation) of the object into the inertial reference frame of the stationary camera are used to model object behavior. The camera can then be moved along the time axis, raytracing the 4D space, and creating an image collection that can subsequently be composited into a video sequence capturing the time-varying effects.³

In the following sections we will: discuss our fundamental assumptions, and the Minkowski 2D and 3D spacetime diagrams; describe our model, and the construction of 4D objects from 3D objects; and finally, demonstrate the resulting animations of 3D objects in 4D spacetime.

II. THEORY

As pointed out in this journal,⁴ and demonstrated by Terrell⁵ and Penrose,⁶ the visual phenomena we explore here can be described as the combination of a pre-relativistic purely optical effect due to finite lightspeed that was discovered by Roemer in 1677,⁷ and special relativity's four dimensional spacetime discovered by Minkowski in 1908.⁸ The finite speed of light leads to effects analogous to those of sound, as in the case of locating the position of a fast high flying jet by the sound of its engines. Finite and invariant lightspeed requires the physical phenomena predicted by special relativity: time dilation and length contraction. Time dilation is observable only if there is a variation in the object during the viewing period, as in the muon particle's decay. Length contraction is observable by differences in

the geometry of a relativistic object at rest and in motion.

A. Background

Relativistic 4D spacetime (t, x, y, z) consisting of both space and time, is often labeled (3+1)D, referring to three spatial dimensions (x, y, z) and one time dimension t . Similarly, a 3D spacetime (t, x, y) could be referred to as (2+1)D, which is to say containing two spatial dimensions (x, y) and one time dimension t .

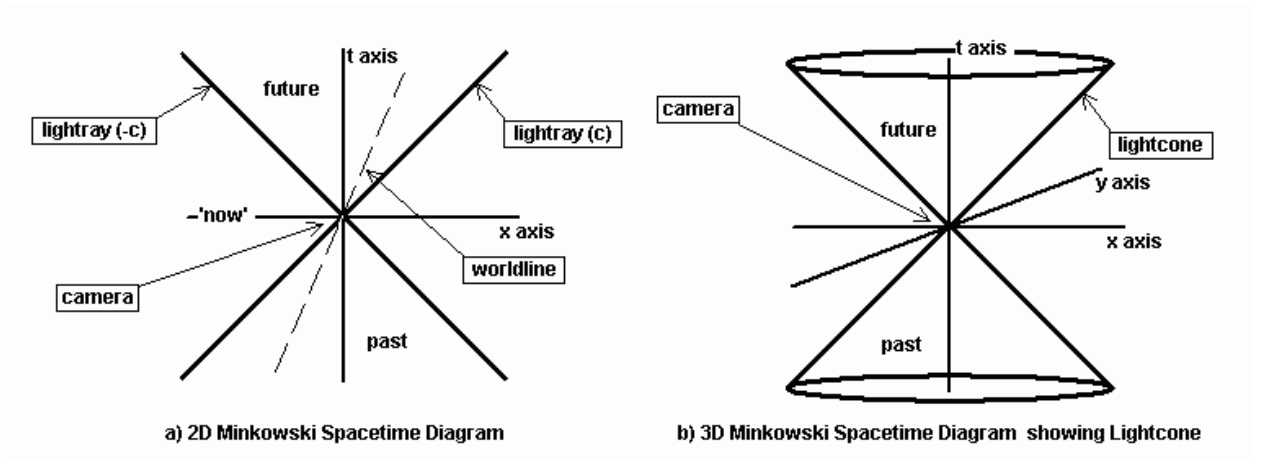


FIG. 1: (1+1)D and (2+1)D Minkowski spacetime diagrams

A camera at the origin can only 'see' an event in the past whose lightray passes from that event through the camera at the origin.

The most convenient units for the purposes discussed here are *relativistic units* where $c = 1$. The benefit of using relativistic units is that the units along all the spacetime axes have the same scale, resulting in a lightray traveling one unit along the spatial axes for each unit it travels along the time axis. A lightray c can thus be represented in a Minkowski 2D spacetime diagram as a 45° bisector, or in a 3D spacetime diagram as the surface of a right circular cone, both shown in Figure 1. We will use the light-second, the distance light travels in a second, as the basic unit of measure in our discussion.

An object's *worldline* is its 4D path through spacetime. The instantaneous direction of an object's worldline is the object's proper time axis. The slope of this proper time axis in the Minkowski diagram represents the object's speed. The worldline through flat spacetime of an object with a constant velocity is a straight line. The normalized tangent to an object's worldline is the object's instantaneous velocity 4-vector.

A 3D object can be created by *extruding*⁹ a 2D object in a direction perpendicular to the 2D plane in which the object lies (for example, by extruding a square from the X, Y plane along the Z axis). Likewise, a 4D object can be created by extruding a 3D object in a direction orthogonal to the 3D hyperplane in which the object lies. A 4D example would be the extrusion of a cube from the X, Y, Z 3-space, along the T axis. Two examples are shown in Figure 2. We call this *temporal extrusion* when a 3D object is extruded along its worldline.

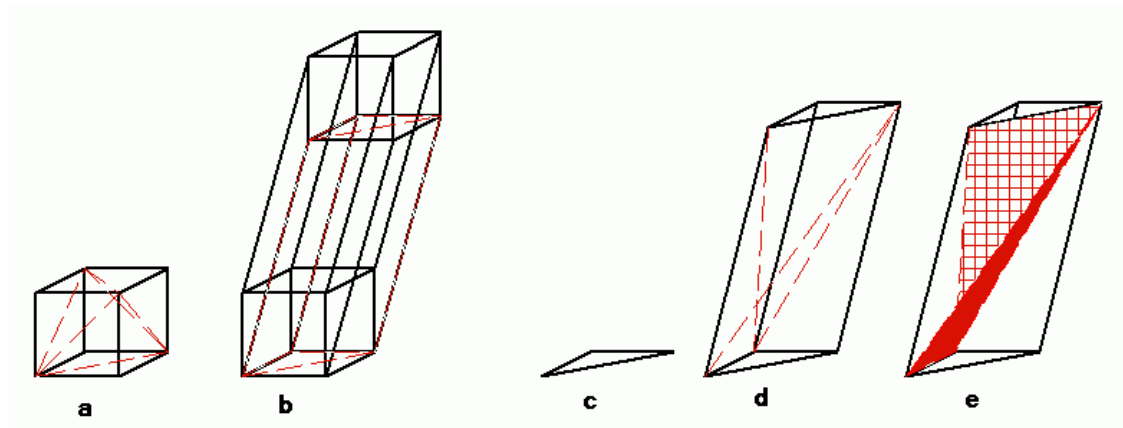


FIG. 2: Cube & triangle: Extruded then tessellated

Raytracing¹⁰ is a geometric 3D image rendering algorithm that colors the pixel on a viewplane by sending a ray from the viewpoint, through a pixel on the viewplane, and out into the scene's 3-space where it may intersect the 2D surface element (such as a triangle) used to define the boundaries of a 3D object. The color of the object's surface at the intersection is used to color the corresponding pixel in the viewplane. This procedure is repeated for each of the pixels in the viewplane. Howard¹¹ adapted the open-source 3D raytracer POV-Ray Version 2.0 to relativistic raytracing by changing the angle of incidence as a light ray passes from one inertial reference frame to another. We found it necessary to increase the model's flexibility in order to demonstrate the difference between finite lightspeed effects and relativistic effects.

We have developed a simple four dimensional raytracer by globally extending a 3D raytracer's¹² vector math from 3D to 4D and adding a fourth component t to the coordinate system. We constrained the lightrays to lie on the negative lightcone so the ray travels through the model at lightspeed. The resulting 4D raytracer can image a Euclidean

4D space of 4D objects.

It can be shown that the length of an object with an arbitrary constant relativistic¹³ velocity $\beta = \frac{v}{c}$ will contract in the direction of motion by a factor of $\frac{1}{\gamma} = \sqrt{1 - \beta^2}$. It can also be shown that the proper duration between any two events on the relativistic object's worldline will expand (dilate) by the Lorentz factor $\gamma = \frac{1}{\sqrt{1 - \beta^2}}$. This is known as **length contraction** and **time dilation**, respectively.

B. Object Construction

Any 3D object defined by bounding triangles such as the cube in Figure 2a can be **temporally extruded** into a 4D hyperobject and inserted in the scene's 4-space by extruding each f of its n individual triangles as follows. Assuming that the triangle's vertices are defined by their 3D coordinates in 3-space, insert a t component into each of the vertex coordinates and set t to some constant value, say t_0 .

$$(x_i, y_i, z_i)_f \rightarrow (t_0, x_i, y_i, z_i)_f.$$

When performed on all three vertices i , the 2D triangle f will have a unique location in 4-space.

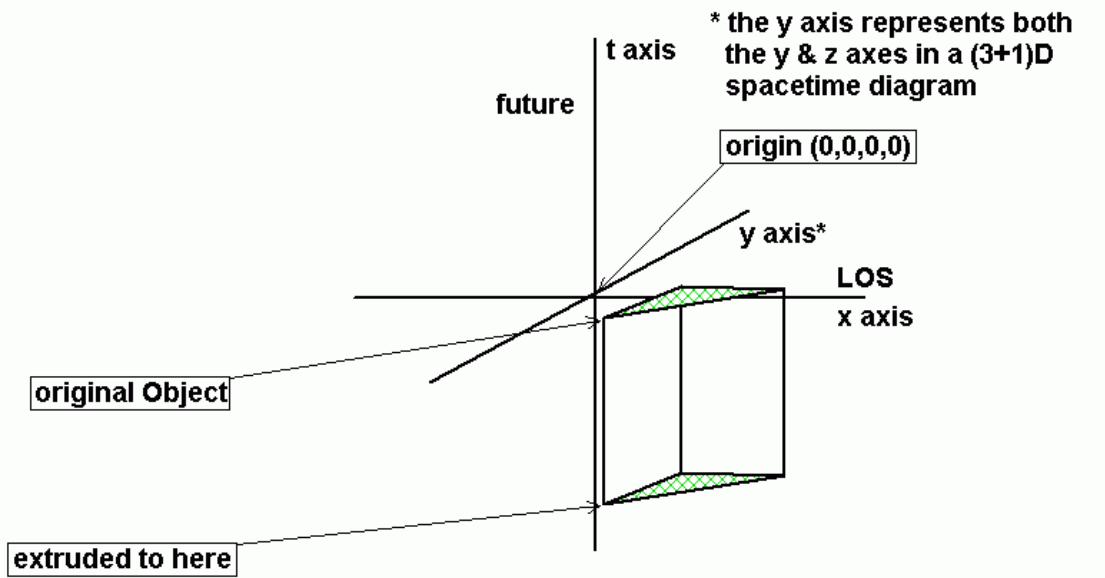


FIG. 3: Temporal extrusion: Triangle at rest extruded into prism

The object now lies embedded in the XYZ hyperplane that is orthogonal to the t axis at t_0 (*original Object* in Figure 3). Each of these triangles f , and hence the object composed from

them, can be extruded into the 4th dimension by duplicating the vertices of the triangles with lesser (or greater) values for the t components. If the object is at rest in the camera frame, a constant Δt can be added to the t component of each of the object's original triangles in the t_0 hypersurface to create an f' duplicate triangle to be used as the object's position in the $t_0 + \Delta t$ hypersurface.

$$(t_1, x_i, y_i, z_i)_{f'} = (t_0, x_i, y_i, z_i)_f + (\Delta t, 0, 0, 0) \quad (1)$$

Where $f = \{1..n\}$ refers to each of the original triangles, $f' = n + \{1..n\}$ to each of the corresponding extruded triangles, and $i = \{1, 2, 3\}$ to each of the corresponding vertices that define each triangle pair.

As shown in Figure 3 where $\Delta t < 0$, connecting the three vertices ($i = 1, 2, 3$ in Eqn 1) of the original triangle f with the respective vertices of the extruded triangle f' creates a 3D prism from the original triangle. Thus the triangle f exists only between t_0 and t_1 , inclusive.

The prisms are then tessellated¹⁴ into three adjacent tetrahedra as shown in Figure 2e. The 3D simplices are necessary for the barycentric algorithm (described below) used to determine where, on the 3-manifold surface of the 4D object the intersection with the lightray occurs.

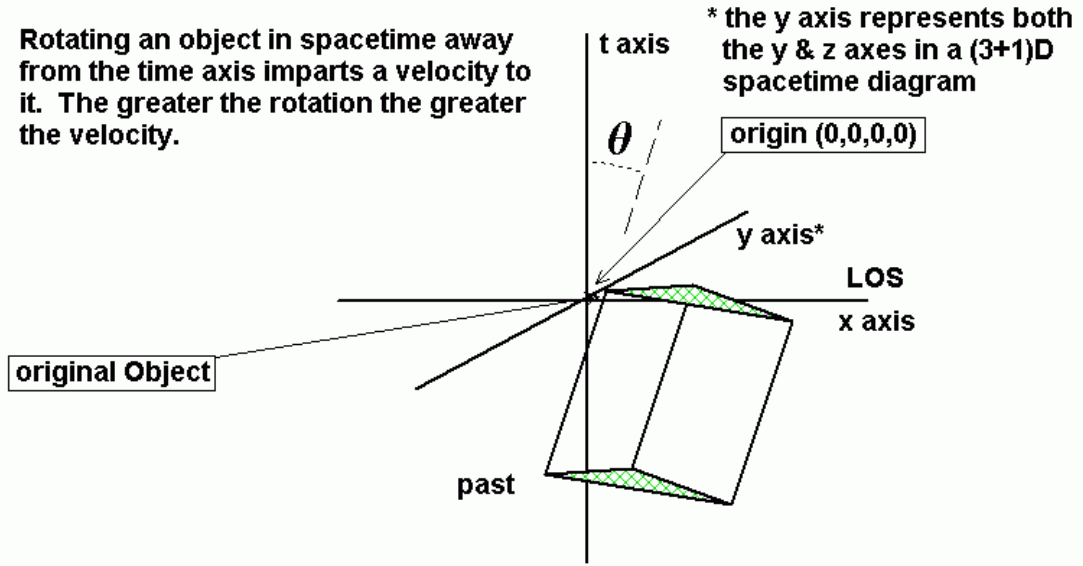


FIG. 4: Temporal extrusion not parallel to 't' axis

$$\text{Object has moved: } velocity = \frac{\Delta x}{\Delta t}$$

An object's velocity is represented by changing the position of the extruded end of the triangle (Figure 4) with respect to the original end: $x_{end} = x_{beg} + \Delta x$ spatial units. The speed in the camera frame would thus be $\frac{\Delta x}{\Delta t} \frac{\text{spatial units}}{\text{time unit}}$. Canceling the units yields the dimensionless fraction $\frac{\Delta x}{\Delta t}$. A lightray's slope $c = \pm 1.0$ is represented by both the diagonal lines and the surface of the lightcone of Figure 1. For the general 3D case, where the distance traveled in time Δt is $\Delta d = \sqrt{\Delta x^2 + \Delta y^2 + \Delta z^2}$, the speed would be $\frac{\Delta d}{\Delta t}$, and Eqn 1 would become:

$$(t_1, x_i, y_i, z_i)_{f'} = (t_0, x_i, y_i, z_i)_f + (\Delta t, \Delta x, \Delta y, \Delta z) \quad (2)$$

C. Viewing 3D Objects in (3+1)D Spacetime

Consider a camera at the origin, whose line-of-sight (LOS) is collinear with the x axis. Since a lightray's worldline as depicted in the spacetime diagram lies on the lightcone, an object must cross the lightcone in the diagram in order to be visible to the camera. In fact, the object is visible to the camera only while it is intersecting that lightcone whose apex is coincident with the camera (assuming the camera is pointing at the object) as shown in Figure 5.

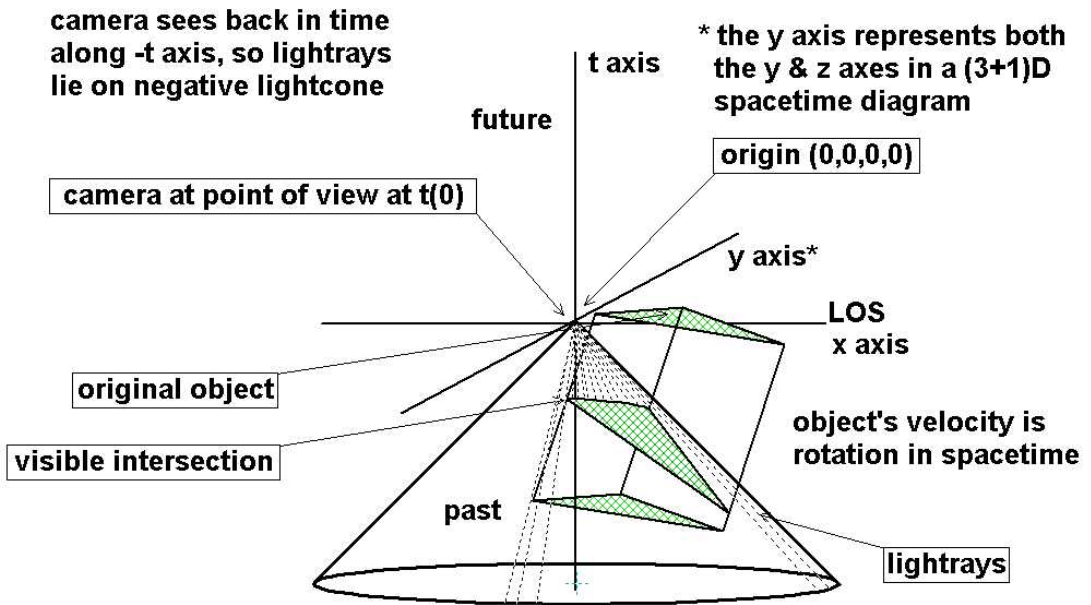


FIG. 5: Temporal extrusion of moving object with lightcone

A non-relativistic spacetime: finite lightspeed but no Lorentz transform

Figure 5 depicts a right circular hypercone in 4-space, whose symmetric axis is collinear with the $-t$ axis, and whose apex is coincident with the camera at the origin $(0,0,0,0)$. This hypercone's hypersurface, depicted by the inverted cone, has 3 dimensions, sufficient to contain the camera's focal point and the lightrays entering its lens. Although a 3-manifold in 4-space, this hypercone is known as a **lightcone**. A lightcone is thus the locus of all points that satisfy:

$$(t_p, x_p, y_p, z_p) = (-\sqrt{x_p^2 + y_p^2 + z_p^2}, x_p, y_p, z_p) \quad (3)$$

Note that the light travels from the object to the lightcone's apex at the origin. As depicted by the broken lines representing lightrays in Figure 5, a camera located at the apex in this 4D model can see only those 3D objects whose extruded triangles (tetrahedra triads) intersect the lightcone. The only visible objects are those with vertex extrusion pairs (t_0, x_i, y_i, z_i) of the original object and (t_1, x_i, y_i, z_i) of its extruded end-cap, where

$$t_0 \geq \sqrt{x_i^2 + y_i^2 + z_i^2} \geq t_1, \forall \{(t_0, x_i, y_i, z_i) \ \& \ (t_1, x_i, y_i, z_i)\} \quad (4)$$

The intersecting portion of the extruded triangle is depicted by the triangle labeled *visible intersection* in Figure 5. Note that geometric distortion in the object is caused by the intersection of the triangle and the lightcone. An object in the lightcone is easily detected since a straight line can be intersected with a 3D object in Euclidean 4-space in the same manner as a straight line is intersected with a 2D object in 3-space.

D. Animating Spacetime Objects

There is no mathematical or geometric limit to an object's speed in the model, its velocity being the slope of the temporal extrusion vector. For real physical objects, some physical mechanism must accelerate the object to the speed with which the object enters the model's laboratory inertial frame. We can assume with some confidence that this speed must be less than that of light. The physical objects will then maintain an extrusion vector with a $\frac{|\Delta x|}{\Delta t}$ slope of less than 1.0, or an angle of less than 45° with respect to the t axis on the Minkowski diagram as shown by θ in Figure 4. Since we are considering only uniformly moving objects, we can ignore the specifics of the spacetime rotation that yield the extrusion angle.¹⁵

Two classes of 4D objects have been implemented: one for the finite lightspeed objects and one for relativistic objects. The first is inserted into the scene without length contraction or time dilation as shown in Figure 5, and the second is inserted with the Lorentz transformation

as shown in Figure 6. Conceptually, the former may be considered to have been measured in the laboratory inertial reference frame's subjective units (it was already length-contracted and time-dilated), while in the latter case the object was measured in its own rest frame. The relativistic objects therefore must be length contracted and time dilated prior to insertion.

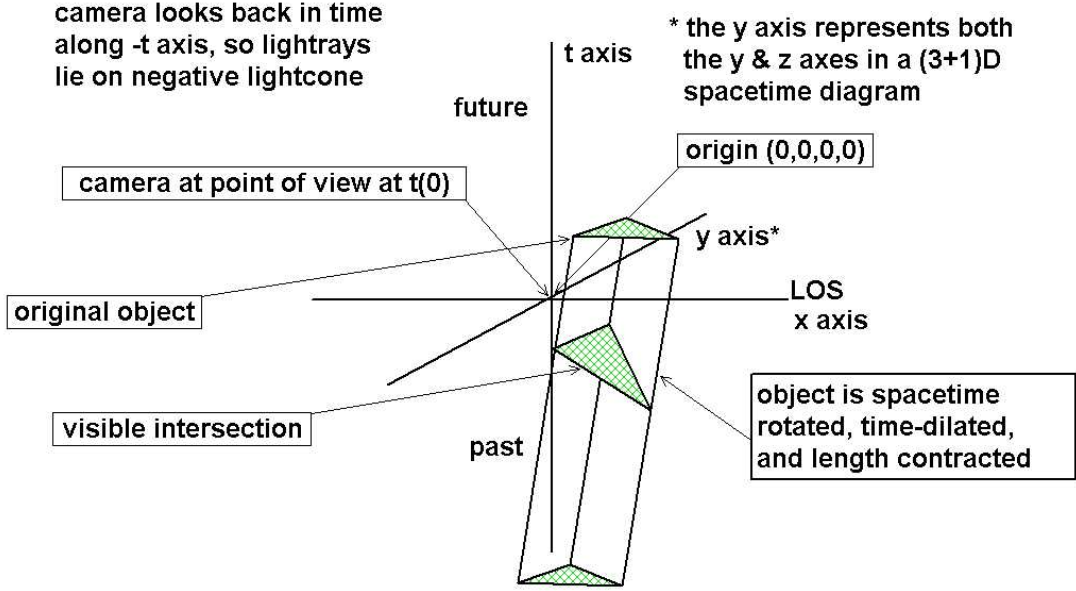


FIG. 6: Lorentz transformed object

A velocity in the neighborhood of 86.6% of c yields a γ factor around 2. The prism is shown length contracted by $\sim \frac{1}{2}$ and its proper time axis is dilated by ~ 2

The animation procedure is straight forward. For example, to generate 20 seconds of animation at 10 frames per second ($\Delta t = 0.1seconds$), the procedure is as follows.

1. Beginning with the camera at (t_0, x_0, y_0, z_0) , a view is rendered and saved.
2. The camera is moved forward in time to (t_i, x_0, y_0, z_0) , where $t_i = t_{i-1} + \Delta t$ and the view is rendered and saved;
3. Repeat from step 2 while $t_i < 20$.

Notice that the camera's spatial components (x, y, z) do not change, only the time component of the camera position. Crucial to the simplicity of the procedure is the fact that the 4D object's bounding surfaces (and the tessellating tetrahedra that comprise those surfaces) **do not change**. The 4D world is **static**. Only the point of intersection of the lightcone changes as the camera and its lightcone progress along the t axis.

E. 4D Intersection Algorithm

Lightcone crossing events are detected by solving for the intersection of a lightray with each of an object's bounding tetrahedra. The set of lightrays is defined as that set of 4D straight lines passing from the camera through each of the pixels in the viewplane's pixel grid and out into 4D space. Using a 4D implementation of the barycentric algorithm to compute the intersections of the ray with all tetrahedra faces, we select the intersecting event nearest to the camera (with the t value closest to 0.0). The array of 1D lightrays that originate from the gridded viewplane results in a 2D image of the objects projected onto that viewplane.

Since the objects have been Lorentz transformed prior to the intersection, such that their geometry is correct for the camera frame in which the intersection occurs, the geometric components of the lighting model, the surface normal and the reflection angle, can be used to approximate the pixel shade just as with a conventional lighting model in 3D rendering.

Photorealistic rendering requires the addition of lighting effects such as Doppler shift¹⁶ and the searchlight effect, which could dominate the rendered image and obscure the visualization of the object's geometry.¹⁷ For this reason, these effects were not implemented in this model.

III. RESULTS

Three models of relativistic motion are displayed in the sequential images in Figure 7. The object displayed is a flange (angle bracket) 2 light-seconds wide by 2 light-seconds deep by 4 light-seconds tall. Its thickness is negligible (being constructed of four 2D triangles). The top row shows the traditional ray-tracing technique, where the lightspeed is effectively infinite. In the middle row, the pre-relativistic optical effects are shown, while in the bottom row, the relativistic effects are displayed. The finite lightspeed camera (top row) was moved ahead in time 18.675 seconds, an amount equal to the lightspeed delay from the center of the stage to the camera, so that the flanges appear to be in approximately the same positions.

The scene is set upon a stage with an overhead light source, both at rest in the camera frame. Two flanges approach, cross, and depart the centerline of the scene at $0.866c$. The geometric distortions of the center row are due exclusively to classical aberration. Those of

the third row are due to relativistic aberration.

The stage's mirrored backdrop shows the reflections of the flanges from behind. Note the difference in the positions of the reflections in the three rows. The top row shows the instantaneous reflections of the flanges, while the middle and bottom rows show the retarded reflections due to the lightspeed delay imposed by the added distance to be traveled by the lightray from the object to the mirror and back. The distances modeled are on the order of the size of the Jovian system.¹⁸

Note the bottom flanges *appear* to cross each other before the top flanges. Note also, that even with this head start, the top flanges arrive at their respective edges at the same time as the bottom flanges. The bottom flanges appear to approach faster and retreat slower than the top flanges. This is the visual evidence of the pre-relativistic optical effect known as classical aberration. The flanges approaching the centerline of the stage are obliquely approaching the camera. Aberration causes the angle from the centerline to the flanges to appear smaller than the proper angle of incidence, resulting in the object appearing closer to the centerline, or ahead of the object's proper position as depicted in the top view.

This is true for both the leading and the trailing edges of the flange, independently. As a result, the leading edge, which is closer to the centerline, appears to have moved further than the trailing edge, giving the impression of a wider flange. The opposite effect occurs as the flanges move away from the centerline. The flanges appear to incrementally speed up and simultaneously contract as they move relativistically away from the camera. These aberration effects are apparent in the bottom two images of Figure 7.

IV. CONCLUSIONS

This paper has visually demonstrated that implementing a simple algorithm that consists of a finite lightspeed component and a length contraction component yields special relativistic visualizations similar to those using more complex visualization systems.¹⁹ We have viewed the difference between pre-relativistic optical effects due to a finite lightspeed and those effects predicted by special relativity.

We have demonstrated that 3D animated sequences can be generated from a static 4D Euclidean spacetime. Furthermore, we have demonstrated that 3-space can be visualized as the intersection of a lightcone and Euclidean 4-space, where the slope of the lightcone's

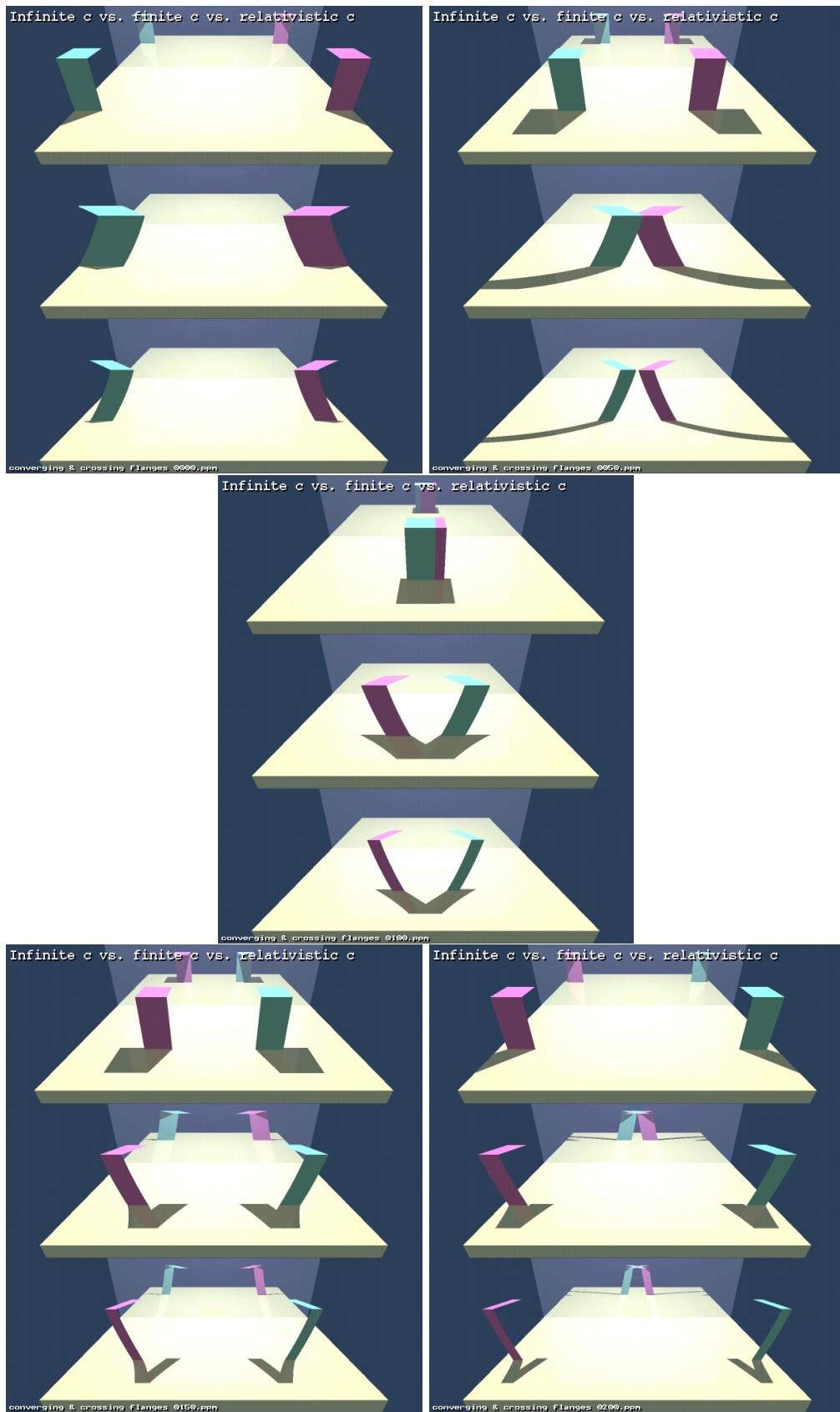


FIG. 7: Sequential images of two 4D objects converging then crossing at $0.866c$ on a mirrored background

Top row: infinite lightspeed 4D raytracing;
 Center row: pre-relativistic spacetime model;
 Bottom row: relativistic spacetime model

hypersurface determines the constant lightspeed in the model. The model has been described using only algebra and Euclidean geometry.

Acknowledgements

We would like to thank Dr. Daniel Weiskopf and Dr. Arvind Rajaraman for their invaluable comments and suggestions. A special thanks also to Dr. James Arvo for his ToyTracer raytrace kernel code.

* Electronic address: dblack@uci.edu

† Electronic address: gopi@uci.edu

‡ Electronic address: fwessel@uci.edu

§ Electronic address: pajarola@acm.org

¶ Electronic address: fkuester@ucsd.edu

¹ *Temporal homogeneity* implies the object’s visible elements do not change during the viewing period. Object shape, color, size, attitude, as well as velocity, are constant.

² *Flat spacetime* is not curved - objects obey Newton’s Laws, and a geodesic (straight line) is straight.

³ D. V. Black, “Viewing classical and relativistic spacetime”, Supporting video sequences, <http://www.hypervisualization.com/videos/black/> (World Wide Web, 2004).

⁴ R. J. Deissler, “The appearance, apparent speed, and removal of optical effects for relativistically moving objects”, *Am. J. Phys.* **73**, 663–669 (2005).

⁵ J. Terrell, “Invisibility of the lorentz contraction”, *Phys. Rev.* **116**(4), 1041–1045 (1959).

⁶ R. Penrose, “The apparent shape of a relativistically moving sphere”, *Pro. Cambridge Philos. Soc.* **55**, 137–139 (1959).

⁷ O. Roemer, “A demonstration concerning the speed of light”, *Philos. Trans. R. Soc. London* **136**, 893–894 (1677).

⁸ H.A. Lorentz, A. Einstein, H. Minkowski, and H. Weyl, *The Principle of Relativity* (Dover Publications, 1923), pp. 73–91.

⁹ *Extrusion* is a Computer Aided Design (CAD) construction operation that converts an n

dimensional object into an $n + 1$ dimensional object. The vertices, edges, and faces of the object are all extruded into the next higher dimension along the extrusion vector and then connected by edges, planes and prisms, respectively.

- ¹⁰ A. S. Glassner, *An introduction to ray tracing* (Academic Press Limited, San Diego, CA, 1989).
- ¹¹ A. Howard, S. Dance, and L. Kitchen, *Relativistic ray-tracing: simulating the visual appearance of rapidly moving objects* Technical Report 95/21, (The University of Melbourne, July 1995), pp. 1–13.
- ¹² D. Kirk and J. Arvo, “The ray tracing kernel”, In *Proceedings of Ausgraph* (Melbourne, Australia, 1988), pp. 75–82.
- ¹³ **Relativistic velocity** is used to describe the relative speeds between two referents of $0.866c$ or greater. The adjective **relativistic** also describes an object that is moving with relativistic velocity with respect to the camera frame in which the observer is at rest.
- ¹⁴ **Tessellated** is used to describe a hyperplane (e.g. a prism) tiled with a pattern (e.g. a tetrahedra) in such a way as to leave no region uncovered. The covering hyper-tiles (tetrahedra) need be neither regular nor congruent.
- ¹⁵ The temporal homogeneity assumption obviates the need for a discussion of hyperbolic rotation.
- ¹⁶ P-K Hsiung, R.H. Thibadeau, C.B. Cox, R.H.P. Dunn, M. Wu, and P.A. Olbrich, “Wide-band relativistic doppler effect visualization”, In *IEEE Visualization 1990 Proceedings* (IEEE, 1990), pp. 83–92.
- ¹⁷ D. Weiskopf, U. Kraus, and H. Ruder, “Searchlight and doppler effects in the visualization of special relativity: A corrected derivation of the transformation of radiance”, *ACM Trans. Graph.* **18**(3), 278–292 (1999).
- ¹⁸ At the recorded animation rate (your playback may differ), the size of the stage is about 6 million Km on a side (20 light-seconds), easily large enough to encompass the planet Jupiter and the orbits of its four largest moons.
- ¹⁹ D. Weiskopf, M. Borchers, T. Ertl, M. Falk, O. Fechtig, R. Frank, F. Grave, P. Jezler, A. King, U. Kraus, et al., “Visualization in the Einstein Year 2005: A Case Study on Explanatory and Illustrative Visualization of Relativity and Astrophysics”, In *IEEE Visualization 2005 Proceedings* (IEEE, 2005), pp. 583–590.